Conclusion

The perturbing influence of solvent (or probe) on the value of the polymer–polymer interaction parameter (χ), and the differences in χ values obtained by means of different experimental techniques, can be effectively minimized using the method of calculation of χ here proposed, which is based on equation-of-state *ternary* theory. This conclusion holds for the typical polymer pair here studied but should be extended to other systems (especially those having larger free-volume differences).

Acknowledgment. This work has been supported by CICYT, Spain, under Projects No. PB86-566 and PA87-705.

Registry No. PS, 9003-53-6; PVME, 9003-09-2; C_6H_6, 71-43-2; Cl_3CH, 67-66-3; hexane, 110-54-3; heptane, 142-82-5; octane, 111-65-9; 2,2,4,4-tetramethylpentane, 1070-87-7; cyclopentane, 287-92-3; cyclohexane, 110-82-7; toluene, 108-88-3; isopropyl ether, 108-20-3; *p*-dioxane, 123-91-1; propyl acetate, 109-60-4; acetone, 67-64-1; 2-butanone, 78-93-3; carbon tetrachloride, 56-23-5; dichloromethane, 75-09-2; tetrachloroethene, 127-18-4; trichloroethene, 79-01-6; fluorobenzene, 462-06-6.

References and Notes

(1) Preliminary reports of this work in: (a) *Abstracts*, 31st Macromolecular Symposium, Merseburg, Germany, June 30–July 4, 1987; p 231 (Microsymposia IV and V). (b) *Actas*, 1st Latin American Symposium on Polymers, Porlamar, Venezuela, July 24–29, 1988; Vol. 2, p 1259.
(2) Olabisi, O.; Robeson, L. E.; Shaw, M. T. *Polymer–Polymer Miscibility*; Academic Press: New York, 1979.
(3) Paul, D. R., Newman, S., Eds. *Polymer Blends*; Academic Press: New York, 1978.
(4) Flory, P. J. *Principles of Polymer Chemistry*; Cornell University Press: Ithaca, NY, 1953.
(5) Riedl, B.; Prud'homme, R. E. *Polym. Eng. Sci.* **1984**, *24*, 1291.
(6) Walsh, D. J.; Rostami, S. *Adv. Polym. Sci.* **1985**, *70*, 119.
(7) Klotz, S.; Schuster, R. H.; Cantow, H. J. *Makromol. Chem.* **1986**, *187*, 1491.
(8) Nandi, A. K.; Mandal, B. M.; Bhattacharyya, S. *Macromolecules* **1986**, *19*, 1478.
(9) Huggins, M. L. *Ann. N.Y. Acad. Sci.* **1942**, *43*, 9.
(10) Flory, P. J. *Proc. R. Soc. London, Ser. A* **1942**, *234*, 60.
(11) Masegosa, R. M.; Prolongo, M. G.; Horta, A. *Macromolecules* **1986**, *19*, 1478.
(12) Scott, R. L. *J. Chem. Phys.* **1949**, *17*, 249.
(13) Horta, A. *Macromolecules* **1985**, *18*, 2499.
(14) Horta, A. *Macromolecules* **1989**, *22*, 2009.
(15) Desphande, D. D.; Patterson, D.; Schreiber, H. P.; Su, C. S. *Macromolecules* **1974**, *7*, 530.
(16) Eichinger, B. E.; Flory, P. J. *Trans. Faraday Soc.* **1968**, *64*, 2035.
(17) Al-Saigh, Z. Y.; Munk, P. *Macromolecules* **1984**, *17*, 803.
(18) $\kappa = (V_2^*/V_1^*)\{\Gamma/\xi_2\xi_3 + \chi_{12}(\tilde{V}_2/\tilde{V}_{23} - 1)[\xi_3^{-1} + (s_2 - s_3)/(\xi_2 s_2 + \xi_3 s_3)] + \chi_{13}(\tilde{V}_3/\tilde{V}_{23} - 1)[\xi_2^{-1} - (s_2 - s_3)/(\xi_2 s_2 + \xi_3 s_3)]\}$ with Γ of eq 10 taken at $\phi_p \to 1$.
(19) Panayiotou, C.; Vera, J. H. *Polym. J.* **1984**, *16*, 89.
(20) Panayiotou, C.; Vera, J. H. *Polym. J.* **1984**, *16*, 103.
(21) Hadziioannou, G.; Stein, R. S. *Macromolecules* **1984**, *17*, 567.
(22) Shibayama, M.; Yang, H.; Stein, R. S.; Han, C. C. *Macromolecules* **1985**, *18*, 2179.
(23) Han, C. C.; Bauer, B. J.; Clark, J. C.; Muroga, Y.; Matsushita, Y.; Okada, M.; Tran-cong, Q.; Chang, T.; Sanchez, I. C. *Polymer* **1988**, *29*, 2002.
(24) Su, C. S.; Patterson, D. *Macromolecules* **1977**, *10*, 708.
(25) Bondi, A. *Physical Properties of Molecular Crystals, Liquids and Glasses*; Wiley: New York, 1968.

Melting and Crystallization Kinetics of a High Molecular Weight *n*-Alkane: $C_{192}H_{386}$

G. M. Stack

Naval Research Lab, USRD, P.O. Box 8337, Orlando, Florida 32856

L. Mandelkern*

Department of Chemistry and Institute of Molecular Biophysics, Florida State University, Tallahassee, Florida 32306

C. Kröhnke

CIBA-GEIGY AG, NTL 2441, CH-4002 Basel, Switzerland

G. Wegner

Max-Planck-Institut fur Polymerforschung, Jakob-Welder-Weg 11, D-6500 Mainz, West Germany. *Received August 29, 1988; Revised Manuscript Received April 7, 1989*

ABSTRACT: The fusion process and the crystallization kinetics from the pure melt of the *n*-alkane $C_{192}H_{386}$ have been studied. Several fundamental features of these processes have emerged. At room temperature the compound is completely crystalline, consistent with the formation of molecular crystals, while premelting is observed at elevated temperatures. A theoretical basis is presented for the premelting. The possibility of premelting in the other *n*-alkanes suggests the need to reexamine the analysis of the melting temperature–composition relations for such species. The crystallization kinetics from the pure melt obey classical theory. The temperature coefficient of the crystallization process indicates that it is nucleation controlled and follows the theory developed for chains of finite molecular weight. Analysis of this kinetic data allows for a connection to be made between the crystallization of low and high molecular weight chains.

Introduction

The recent synthesis of very high molecular weight *n*-alkanes[1-3] has provided a set of model compounds whose study will allow for a further understanding of the fusion–crystallization process in general and that of polymers in particular. Studies with these compounds can serve as a bridge to the crystallization behavior of polymers by comparing the characteristics of these *n*-alkanes with low molecular weight linear polyethylene fractions crystallized from either the bulk or from dilute solution.[4-8] Comparable molecular weights from both classes of compounds are now available. The very close connection between the

0024-9297/89/2222-4351$01.50/0

two types can be seen in the fact that the molecular weight at which folding occurs, for crystallization from either the bulk or dilute solution, is the same for the *n*-alkanes and the fractions of linear polyethylene.[4-7,9]

Analysis and study of the high molecular weight *n*-alkanes concerned with nucleation theory,[9,11] morphology,[10,12-14] and crystallization kinetics[15] have recently appeared. The major emphasis in much of these works has been an effort to elucidate the nature of the interfacial structure and to establish the relationship between the crystallite thickness and the extended molecular length.

In the present work, involving studies with dononacontahectane, $C_{192}H_{386}$, we focus our attention instead on the fusion process and the crystallization kinetics from the pure melt. An understanding of these two fundamental processes should provide the proper framework for the investigation of other factors such as morphological features, the interfacial structure, and the relative crystallite thickness. These latter properties, albeit very important ones, will not be directly addressed in the present work. We will direct our attention to the two basic phenomena stated above.

Experimental Section

Thermal analysis experiments were performed using a Perkin-Elmer differential scanning calorimeter (DSC-4). Sample sizes were of the order of 1 mg, and a series of heating rates from 0.2–10 °C/min were employed. Isothermal crystallizations were performed directly in the calorimeter by first melting the samples at 130 °C for several minutes and then rapidly cooling to the desired crystallization temperature. Static calibration of the crystallization temperatures was performed by melting an Indium standard at 0.5 °C/min. The observed melting peaks were further corrected by heating rate studies as described in the Results and Discussion.

The crystallization kinetic data were obtained by utilizing one of two procedures. In one method the exothermic peak was recorded while the sample was maintained at the isothermal temperature. This peak was then integrated to various crystallization times. In the other method the samples were heated subsequent to isothermal crystallization for a fixed time. The area of the resulting endothermic melting peak was then used to determine the amount of crystallinity that had developed.

The purity of the dononacontahectane used here is very important in assessing the experimental results. The basic method that was used to synthesize the higher molecular weight *n*-alkanes has been previously described.[3,16] The synthetic strategy that was used is based on the oxidative oligomerization of an α,ω-diethynylalkane with 24 carbon atoms. The oligomers of general formula I were then hydrogenated as described previously over a Pd/C catalyst to yield the desired *n*-alkanes.[16] The major

$$HC{\equiv}C(CH_2)_{20}C{\equiv}C{-}C{\equiv}C(CH_2)_{20}C{\equiv}CH$$

I

impurities that could effect the crystallization and melting behavior of the *n*-alkanes could be of the following origin: (a) presence of oligomers with larger or smaller chain length; (b) presence of cyclic products; (c) structural irregularities; (d) added impurities.

Since the different oligomers of the polymer homologous series I differ sufficiently in size and adsorptivity from each other, they can be easily separated by column chromatography as previously described, giving pure fractions of individual oligomers terminated by acetylene groups.

The purity of the fractions was checked by HPLC in each case. The separation of the intermediate oligodiynes was carried out by HPLC on a preparative scale using a Bischoff column (length 25 cm, diameter 4 cm) filled with silica gel Liquosorb Si 1000 (particle size 5 μm). The mixture was chromatographed after dissolving in a mixture of cyclohexane with 3.5–5% 1,4-dichlorobutane with a pressure of 60 bar and a flow of 15 mL/min at 50 °C. The appearance of the individual oligomers was monitored by UV detection (λ = 240 nm). Purity with regard

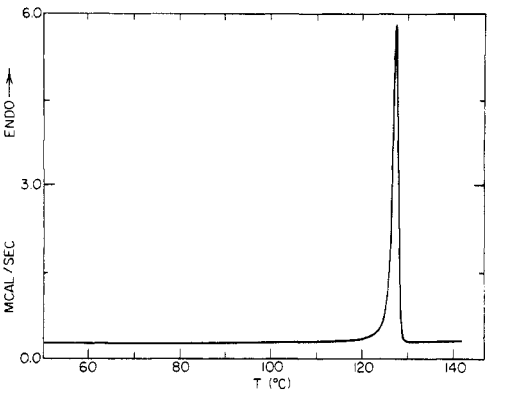

Figure 1. Differential scanning calorimetric thermogram for $C_{192}H_{386}$ isothermally crystallized at 117.5 °C.

to chain length distribution depends then entirely on the purity of the starting 1,3-tetracosadiyne, which was checked by NMR spectroscopy. No shorter or longer chain length material was present in this substrate. Hydrogenation of I will not change the chain length, and thus the *n*-alkanes derived from I must have the same number of C atoms as the starting material.

Oxidative oligomerization of oligomers I leads to formation of cyclic oligomers as byproducts as described previously.[3,16] The cyclic products of structure II differ in their elution behavior from

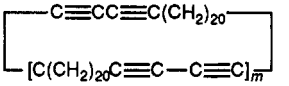

II

the linear products I and can be easily identified in either conventional column chromatography (Al_2O_3/cyclohexane) or GPC.[16] During the purification of the linear oligomers by chromatography the cyclic byproducts were fractionated off. Furthermore, in a separate set of experiments it was proven that cyclic *n*-alkanes and linear *n*-alkanes do not cocrystallize. Since all *n*-alkanes were recrystallized several times, in order to remove the last traces of catalyst of the hydrogenation, cyclic impurities are not expected to be present.

The hydrogenation of terminal and interior acetylene groups was proven to be quantitative by the total disappearance of the IR and Raman bands of these groups. Moreover, the IR and Raman spectra of the oligomer *n*-alkanes contained *all* bands known to belong to *linear* *n*-alkanes and *no* extra bands.[3,17] Thus all bands could be unambiguously identified. Thus structural irregularites cannot be present within the detection limit of IR spectroscopy. This statement is particularly important with regard to the possible presence of multiple bonds from incomplete hydrogenation. The presence of such defects would have been detected with great sensitivity by IR spectroscopy. The spectra of our *n*-alkanes published elsewhere[16,17] do not show such features.

Solvents used to recrystallize the *n*-alkanes (petroleum ether of bp 80–100 °C, *o*-xylene) can always be a source of unspecific added impurities. Rigorous drying of the material in vacuo until constant weight is reached was helpful to establish the purity. Furthermore, IR spectra (KBr disks) did not show the presence of *o*-xylene when the latter was used as solvent for recrystallization. About 20 mg of dononacontahectane was available for this study.

Results and Discussion

Raman internal mode measurements[18-20] of $C_{192}2H_{386}$ samples, which have either been isothermally crystallized or slowly cooled from the pure melt to room temperature, show that they are completely crystalline.[21] The spectra were similar to those obtained for low molecular weight *n*-alkanes.[18,19] Typical results, for a sample crystallized at 114.8 °C for 30 min, are the percent crystalline α_c = 100 ± 5 and the percent liquidlike α_a = 3 ± 2. A DSC thermogram obtained under conventional operating conditions for a specimen isothermally crystallized at 117.5 °C is given in Figure 1. A very sharp, well-defined endothermic peak,

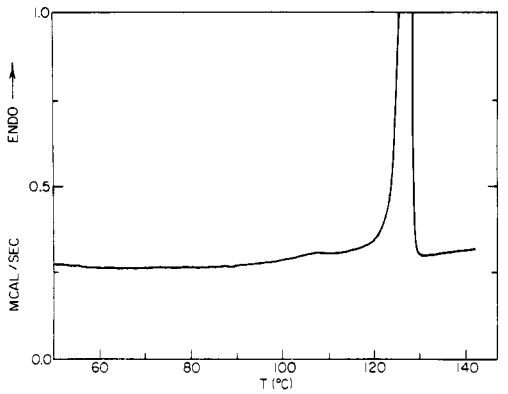

Figure 2. Differential scanning calorimetric thermogram for the same sample as in Figure 1 obtained at higher instrument sensitivity.

as would be expected for a pure compound, is observed. From the area under the endothermic peak the enthalpy of fusion ΔH is found to be 823 cal/mol. This value for ΔH is unexpectedly low based on the expectations for the data on lower molecular weight *n*-alkanes.[22] For example, ΔH for the relatively low molecular weight *n*-alkane $C_{43}H_{88}$ is 800 cal/mol,[22] almost the same as we have obtained for $C_{192}H_{386}$. The Flory–Vrij theoretical analysis[23] fo the *n*-alkane molecular crystals yields an expected value of 940 cal/mol for this compound. Thus, on the basis of the enthalpy of fusion measurements, this high molecular weight *n*-alkane does not appear to be completely crystalline. There is about a 15% deficiency in the number of ordered chain units. On the other hand, the Ramam internal mode analysis gives a completely crystalline system at room temperature. There is then a dilemma in these results that needs to be resolved.

A resolution to this problem can be seen from the DSC thermogram carried out at much higher sensitivity than was used to determine the endotherm in Figure 1. In Figure 2, for the same sample, under the specified conditions, the onset of melting is clearly observed in the vicinity of 90–100 °C. It is clear that some type of premelting has taken place. With this particular experimental technique and sensitivity premelting is observed at about 90 °C. It is possible that with other techniques and greater sensitivity it would be detected at even lower temperatures. The value of ΔH calculated from Figure 2 is 870 cal/mol. This value represents a substantial increase from that obtained from Figure 1. It is about 7% lower than expected theoretical value for a molecular crystal of this chain length. Thus the apparent dilemma between the Raman internal mode data and the enthalpy measurement of Figure 1 is essentially resolved as a consequence of the premelting. The type of premelting that is observed can be given a theoretical basis as will be described below. Moreover, the premelting observed in $C_{192}H_{386}$ is not an isolated phenomenon. Scrutiny of the literature indicates that similar premelting has in fact been observed in other *n*-hydrocarbons although not often recognized as such. We summarize these observations in the following discussion.

Careful dilatometric studies of the fusion of the pure *n*-alkanes, $C_{44}H_{90}$ and $C_{94}H_{190}$, have been reported.[24] The melting temperatures of these two compounds are clearly defined and can be determined very accurately. However, the course of the fusion is different for the two compounds. The $C_{44}H_{90}$ melts according to theoretical expectations and displays an almost classical first-order phase transition. The fusion process is relatively sharp and takes place within an interval of less than 0.25 °C. On the other hand, the fusion of $C_{94}H_{190}$ takes place over a broader temperature range. The onset of melting is observed at 110 °C, and fusion is terminated at 114.5 °C in these dilatometric studies. Premelting is thus observed even in a molecular weight as low as $C_{94}H_{190}$ while $C_{44}H_{90}$ does not show any evidence of premelting by this experimental technique.

Solid-state ^{13}C NMR studies have shown that, for the *n*-alkane octahexacontahectane, $C_{168}H_{338}$, in extended crystalline form, considerable disordering of the end sequence is observed at a temperature well below melting.[25] At 87 °C, about 40 °C below the melting temperature (the only elevated temperature at which spectra were obtained), significant conformational disorder is observed for the terminal CH_3 groups and the adjacent α and β carbons. Although the temperature for the onset of this conformational disorder at the molecular ends was not determined, this observation demonstrates that premelting has taken place well below the melting temperature. This type of conformational disorder was also found in a low molecular weight unfractionated polyethylene as well as in thee "rotator" phase of hexatriacontane.[25] It is thus not a consequence of any structural impurity within the $C_{168}H_{338}$ chain.

In a differential calorimetric study of *n*-hecatane, $C_{100}H_{202}$, Hay reported a major endothermic peak with a heat of fusion of 793 cal/mol.[26] This enthalpy value is obviously quite low for this *n*-alkane. However, also described in this report (without being illustrated) was a "solid-phase transition" at 92 °C, which has 131 cal/mol associated with it. The net enthalpy of fusion is a reasonable value for this *n*-alkane,[22,23] and the lower transition can be interpreted as a premelting phenomenon.

The possibility of premelting also exists during the heating of the *n*-alkane $C_{80}H_{162}$.[27] Here no change in crystal structure is observed nor does any solid–solid transition take place through melting. However, an increase in the long spacing is observed at 90 °C, which is about 20 °C below the melting temperature of the sample. This result could be attributed to premelting. Similarly, the observed reversible change of the intensity of the low-angle maxima in $C_{94}H_{190}$[28] can be assigned to a similar cause.

Ungar and Keller[12] have studied the crystallization from the melt of the *n*-alkane $C_{246}H_{494}$ at elevated isothermal conditions, using small-angle X-rays from a synchrotron source. In order to conclude that a completely extended crystalline form developed, it was necessary to assume that there was a molecular tilt of 35°. If, however, the tilt was in fact slightly less than 35°, then the smaller crystalline thickness could be attributed to conformationally disordered chain ends.

Thus, in addition to the results for $C_{192}H_{386}$ there is other direct, as well as indirect, experimental evidence that premelting occurs in the *n*-alkanes and makes a substantial contribution to the thermodynamic properties. In support of this experimental evidence, a straightforward theoretical basis for this type of premelting in chain molecules is found in the work of Flory and Vrij.[23] In this analysis the collection of chains are taken to be absolutely uniform in length; i.e., they are treated as an ideal monodisperse system. The major portion of their work was concerned with the analysis of fusion from an extreme state of perfect crystalline order to a completely disordered melt. Thus idealized molecular crystals were formed and maintained during the fusion process. However, they also considered the possibility that under favorable circumstances chains with a large but finite number of carbon atoms could exist in some intermediate state of order. They treated in detail the specific situation where the molecular crystals could

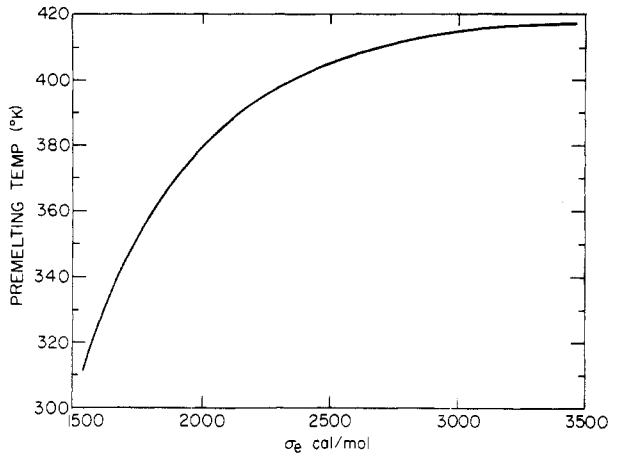

Figure 3. Plot, according to eq 1, of the premelting temperature against interfacial free energy σ_e.

undergo partial melting, involving the disruption of the planar array of the terminal methyl groups, as a prelude to final melting. It is this type of partial melting that is of concern here.

In this calculation m methylene units from the terminal sequence of each molecule are melted. Thus $n-m$ consecutive units from the center of the molecule occupy a crystalline zone comprising similar sequences from neighboring chains. In addition to the free energy of fusion and the interfacial free energies involved, there is also a combinatorial contribution that arises from the number of locations within the molecule that exclude the terminal units from the interior of the crystalline zone. With only these very simple considerations the condition for partial melting at temperature T was found to be given by the inequality[23]

$$\ln\left\{\frac{RT^2}{\Delta H_u \Delta T}\right\} > 1 + \frac{(2\sigma_e + \Delta G_e)}{RT} \tag{1}$$

and the optimum extent of the premelting is given by

$$m^* + 1 = \frac{RT^2}{\Delta H_u \Delta T} \tag{2}$$

In these equations ΔH_u is the enthalpy of fusion per repeating unit, ΔT is $T_m^\circ - T$ where T_m° is the equilibrium melting temperature of the infinite chain. From eq 1 the temperature for the onset of premelting is predicted to depend crucially on the relative values of the quantities σ_e and ΔG_e. The former is the interfacial free energy associated with the boundary between the ordered and disordered region in the premelted chain; ΔG_e is the end-group contribution to the free energy of fusion of the molecular crystal, which can be looked on as the defect free energy for the end-group layers destroyed by partial melting. ΔG_e can be obtained from analysis of the melting of the n-hydrocarbon molecular crystals and is found to be negative.[23] In their analysis Flory and Vrij utilized the best value for σ_e that was available at the time. This corresponded to a value of between 4000 and 5000 cal/mol. When this value was used, it was properly concluded that a temperature very close to T_m° would be required if premelting were to precede final melting. This condition would thus only be met for $n >>> 100$. However, when the premelting temperature is plotted against σ_e, as is illustrated in Figure 3, it is found to be dependent on and very sensitive to the magnitude selected for σ_e. For values of $\sigma_e \geq 3000$ cal/mol premelting is predicted to occur very close to T_m° (418.7 K) in accord with the conclusion of Flory and Vrij. However, as σ_e decreases a precipitous drop

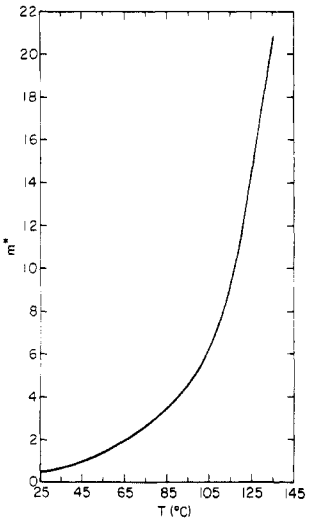

Figure 4. Plot, according to eq 2, of the number of disordered units m^* as a function of temperature.

in the temperature for premelting is predicted. This temperature can be significantly lower than the melting temperature of an n-alkane, particularly for the higher molecular weight homologues. Recent analyses of the melting of equilibrium crystallites of low molecular weight polyethylene fractions indicate values of σ_e that range from 1500 to 3000 cal/mol as the molecular weight increases from 600 to 5000.[6,29] For a molecular weight of 2700, corresponding to $C_{192}H_{386}$, a value of σ_e of 2000 is indicated. This value for σ_e leads to a premelting temperature of 380 K relative to an observed melting temperature of 401 K (see below). Thus the premelting that was observed in Figure 2 is consistent with this analysis. The plot in Figure 3 further suggests that premelting should also occur in the low molecular weight n-alkanes. For a σ_e value of 1500 cal/mol premelting is predicted to occur in the vicinity of 320 K. This temperature is well below the melting point of many of the n-alkanes.

The premelting that is being discussed is clearly specific to chain molecules. It is not among the types that have been usually associated with such systems. This premelting is not caused by an impurity, which reduces the melting temperature and broadens the fusion range, irrespective of molecular structure, as a natural consequence of thermodynamic arguments. It would take an extraordinary impurity content to broaden the fusion range 30–40 °C as is observed here. Neither is this premelting a consequence of chain motion in the crystals of low carbon number n-alkanes, as has been discussed by Ubbelohde,[30] Strobl and co-workers,[31,32] Takimizawa et al.,[27] and Broadhurst[33] and which leads to a variety of solid–solid transformations. Takimizawa et al.[27] have shown that solid–solid transitions take place in the n-alkanes up to $C_{60}H_{122}$. However, at this carbon number and above, solid–solid transitions are not observed.[27,28] We are concerned here with a n-alkane that is well above a carbon number for a solid–solid transition. Thus, the premelting that is observed here does not fall into the category of that discussed for other n-alkane systems. It is, however, consistent with the theoretical expectations.

From the analysis given we can also estimate the number of end disordered units. A plot of m^* against T, calculated from eq 2, is given in Figure 4. Although the amount of disorder predicted by this mechanism is very small at low temperatures, only 1–3 units being involved, it increases rather substantially starting at about 95 °C. At this temperature m^* is aboot 5 units but increases to about 20 units

at 130 °C. For the *n*-alkane of interest in the present work we thus find that a significant number of units from the end of the molecule can be expected to be disordered.

The observed enthalpy of fusion ΔH of $C_{192}H_{386}$ of the major melting peak can be estimated from the expression[23]

$$\Delta H = \frac{(\Delta H_u - \Delta C_p \Delta T)(192 - m^*)}{192} - \frac{\Delta H_e}{192} \quad (3)$$

Here ΔC_p is the specific heat difference between the liquid and crystalline state and ΔH_e is the enthalpy contribution to the interfacial free energy. Taking ΔC_p = 1 cal/mol·deg,[23] ΔT = 17, m^* = 15 units at 125 °C (just below the melting temperature), and ΔH_u = 980 cal/mol,[34] eq 3 becomes

$$\Delta H = 887 - \frac{\Delta H_e}{192} \quad (4)$$

The value expected for ΔH will thus depend on the value of ΔH_e. Flory and Vrij[23] deduced a value of 2150 cal/mol for ΔH_e from the analyses of the melting temperature of the molecular crystals of the *n*-alkanes. For this value of ΔH_e, ΔH equals 876 cal/mol, which is slightly greater than the observed value. However, the correct value for ΔH_e should not be identified with that corresponding to the disruption of the end layers of the *n*-alkane. As the fusion of still higher molecular weight *n*-alkanes is studied, a more reliable value for ΔH_e should be forthcoming and a more direct comparison with eq 4 will be possible.

The experimental results with the *n*-alkane $C_{192}H_{386}$, as well as results in the literature for other *n*-alkanes, give a substantial body of evidence that partial melting, or premelting, involving sequences of units from the ends of the chain takes place prior to melting. The measured enthalpy of fusion of $C_{192}H_{386}$ is quantitatively consistent with premelting and the unpairing of the end groups prior to melting. Experimental results for a series of still higher *n*-alkanes are needed for a more detailed and comprehensive analysis of premelting.

Melting Temperature

A reliable measure of the melting temperatures of the higher molecular weight *n*-alkanes is important for general theoretical concepts and for predicting melting temperatures for similarly constituted polymers.[23] Since only very small amounts of these compounds are available, the melting temperature determination is limited at present to differential scanning calorimetric type measurements. It has already been pointed out that the determination of thermodynamically significant equilibrium melting temperatures of polymers is not obvious by this method.[35,36] The important problems of concern are the sample mass, the heating rate,[35] and the dependence of the observed melting temperature on the crystallization conditions, particularly the temperature.[37,38] It has been shown that constant and thermodynamically meaningful melting temperatures are obtained when sample masses of the order of 1 mg or less are used.[35]

In order to determine the equilibrium melting temperature, we have examined the influence of heating rate on the observed melting temperature of $C_{192}H_{386}$. A typical set of results is given in Figure 5 for a sample crystallized at 121 °C. We find a strong influence of the heating rate, in the higher range, on the observed melting temperature. However, at heating rates of 1 °C/min and less a constant value of T_m of 125.9 ± 0.1 is observed. Higher heating rates give T_m values, which are almost 2 deg higher. Interrupted DSC scans,[35] which yield thermodynamically significant melting temperatures, give a T_m of 125.8 °C for $C_{192}H_{386}$.

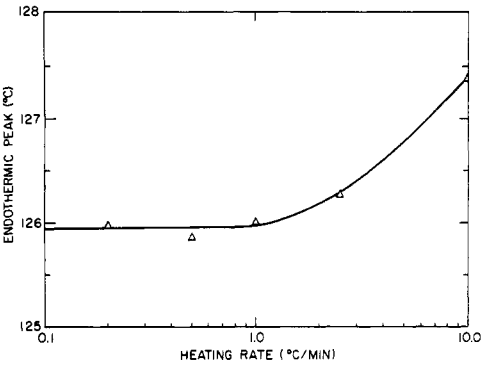

Figure 5. Plot of the location of the endothermic peak as a function of heating rate for a sample of $C_{192}H_{386}$ crystallized isothermally.

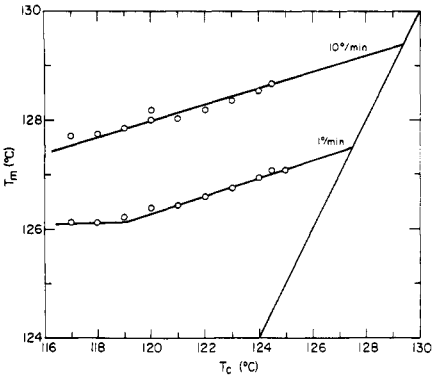

Figure 6. Plot of observed melting temperature against crystallization temperature, T_c, for the two indicated heating rates.

We can conclude, therefore, that heating rates of 1 °C/min or less can give thermodynamically meaningful melting temperatures.

An important question arises as to whether the observed melting temperature depends on the crystallization temperature for this high molecular weight *n*-alkane. This is a well-known and very pronounced effect in the crystallization and melting of polymers.[37,38] It is due primarily to the change in crystallite thickness with crystallization temperature. Since $C_{192}H_{386}$ forms extended-chain type crystallites over the range of isothermal crystallization temperatures, it might be expected that there would be no influence of the crystallization temperature on the melting temperature. However, we have concluded that, even at equilibrium, molecular crystals are not formed at these temperatures. Therefore, the further possibility must be considered that for kinetic reasons equilibrium crystallites are not formed at the crystallization temperature. Therefore, there is the distinct possibility that T_m will depend on the crystallization temperature, and this concern must be addressed by appropriate experiments. The results of such experiments are illustrated in Figure 6. In this figure T_m is plotted against the crystallization temperature T_c for two different heating rates. For both heating rates we find a small but significant influence of the crystallization temperature on the melting temperature that is important in the thermodynamic analysis. The underlying structural basis for this effect is not clear at present. For $C_{192}H_{386}$ we conclude from these observations, utilizing the 1 °C/min heating rate, that the equilibrium melting temperature for $C_{192}H_{386}$ is 127.5 °C.

We can now examine the equilibrium melting temperature determined for $C_{192}H_{386}$ in terms of theoretical expectations. In their analysis of the melting of end-paired molecular crystals of the *n*-alkanes, Flory and Vrij[23] pointed out that although the enthalpy of fusion can be

considered to be a linear function of chain length the corresponding linearity of the entropy of fusion is not valid. Within this end-pairing model for crystals of the *n*-alkanes, they properly calculated the melting temperature–molecular weight relation for these compounds. On the basis of the data then available for the *n*-alkanes and with the tacit assumption that their melting represented the disappearance of the end-paired species, an equilibrium melting temperature of $T_m^\circ = 145 \pm 1$ °C was extrapolated for the infinite molecular weight polyethylene. This conclusion rests crucially on the assumption that the reported melting temperatures in the range C_{50}–C_{100} represented the melting of crystals of completely planar zigzag extended chains, i.e., molecular crystals. With this understanding we can examine the results for $C_{192}H_{386}$ in terms of this theory. Utilizing the parameters appropriate for T_m° = 145.5 °C, T_m for $C_{192}H_{386}$ is found to be 129.5 °C. This temperature is significantly higher than the value determined here.

We have reexamined the Flory–Vrij analysis but limited the data base to *n*-alkanes less than C_{50}. In this range the effect of end disordering should be minimal but cannot be completely ruled out. When the data base is narrowly restricted in this manner, it is found that a wider range of T_m° values can satisfy the requirements of the Flory–Vrij model and theory. In contrast, utilizing the complete data set, up to C_{100}, a T_m° value within 1 deg of 145.5 °C was required for an adequate representation of the data. This result indicates that with a restricted data base it is not possible to obtain a reliable value for T_m° by the Flory–Vrij analysis. Using the parameters appropriate to an arbitrary value for T_m° of 144.5 °C, we find 127.5 °C to be the calculated melting point of a molecular crystal of $C_{192}H_{386}$, a result that is in apparent good agreement with experiment. This agreement is obtained, however, with the model of a molecular crystal being maintained throughout the complete fusion range, i.e., premelting does not occur. However, we have already established that $C_{192}H_{386}$, and presumably the higher *n*-alkanes, do in fact display premelting. Thus, the experimentally determined equilibrium melting temperature is not that required by this aspect of the Flory–Vrij theory. The melting temperature should be higher than that of a molecular crystal since the premelting enhances the thermodynamic stability of the crystalline state.

The melting temperature of chain molecules which, have undergone premelting prior to complete fusion, can also be calculated from another theory given by Flory.[39] When applied to low molecular weight polyethylene fractions, the results depend, as would be expected, on the quantity σ_e.[6,29] Since this quantity has been found to depend on molecular weight a priori predictions cannot be made. However, depending on the relative values of σ_e and ΔG_e, the melting of the end-disordered system could be greater than that for the molecular crystal. This conclusion will also apply to the *n*-alkanes. A more detailed analysis of such systems will involve an investigation of premelting in the lower molecular weight *n*-alkanes (C_{50}–C_{100}) and the determination of thermodynamically significant melting temperatures of the higher molecular weight homologues, which are currently available.

Crystallization Kinetics

The crystallization kinetics from the pure melt were studied utilizing the experimental methods described. The endothermic experiments are most accurate and give the detailed shape and major characteristics of the isotherms. The time scale of these experiments is, however, limited to 1 min or more. More rapid crystallization can be studied using exothermic methods. This method is not accurate for quantifying details of the isotherm shape but is satisfactory for low levels of crystallinity and in establishing the time scale of the crystallization. Utilizing both techniques, we have studied the temperature interval of 115–125 °C. This temperature range encompasses the time for the first detection of crystallinity of about 0.25–200 min. This is essentially the isothermal temperature range accessible to study by calorimetric methods for $C_{192}H_{386}$.[40] Low-frequency Raman acoustical mode (LAM) experiments indicate that extended-chain crystallites are formed at the completion of crystallization at all temperatures in the range studied here.[21]

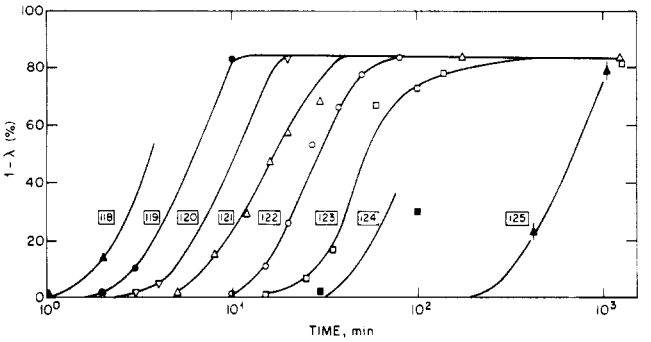

Figure 7. Plot of the degree of crystallinity $1 - \lambda$ against log time for crystallization from pure melt at indicated temperatures.

In Figure 7 we have plotted the degree of crystallinity, $1 - \lambda$, as a function of log time.[41] The data in Figure 7 yield classical Avrami type isotherms typical of the crystallization of monomeric substances as well as long chain molecules.[42-45] Typically, within the experimental error, a set of superposable isotherms along the log time axis is observed. A very strong negative temperature coefficient is observed, suggestive and typical of a nucleation-controlled process.[43-45] For only a 7 deg change in temperature, there is a 4 order of magnitude change in the time for the observation of the onset of crystallinity.

The Avrami equation can be written in its most general form as

$$1 - \lambda(t) = 1 - \exp(-kt^n) \tag{5}$$

which reduces to the free growth, Göler–Sachs expression, at low values of $1 - \lambda(t)$.[46,47] In this equation the nucleation and growth parameters are embodied in the constant n. The parameter k reflects the geometry of the growth and the type of nucleation process that is involved.[43,45] Accordingly, from eq 5 a double logarithmic plot of the experimental data should yield a set of straight lines, with slope n, over the temperature range studied. Such a plot is given in Figure 8 for the data taken from Figure 7. We find that the Avrami relation is followed for about 50–60% of the transformation. This is typical of the results found for low molecular weight polyethylene fractions[45,47] where the Avrami relation is also followed for a relatively high extent of the transformation. A set of parallel straight lines result when the kinetic data are plotted in the indicated manner. The slopes of the straight lines are found to be 4.0 ± 0.2. Previous studies with low molecular weight polyethylene fractions, M = 4200 and M = 5800, also gave a slope of 4 for data analyzed in this manner.[45] Thus, the overall crystallization kinetics of the *n*-alkane $C_{192}H_{386}$ from the pure melt are very similar to, if not identical with, that of low molecular weight polyethylene fractions of comparable chain length. In a strictly formal sense, the exponent n can be taken to represent a homogeneous, or pseudo-homogeneous, nucleation process followed by three-dimensional growth.[43]

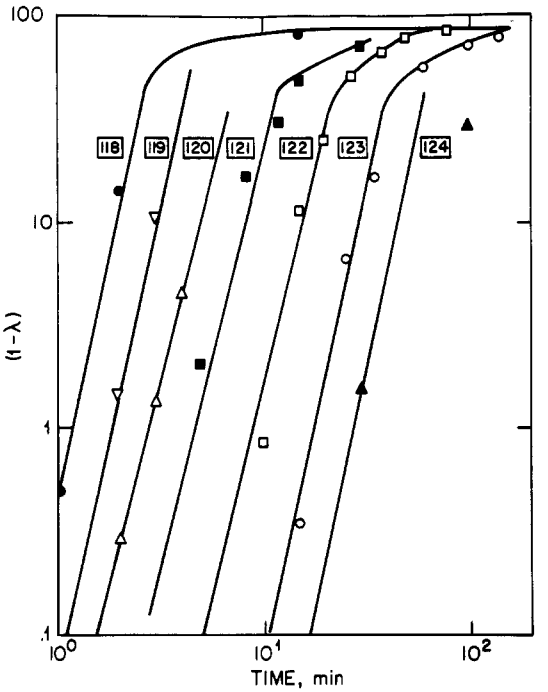

Figure 8. Double logarithmic plot of the degree of crystallinity $1 - \lambda$ against time for data from Figure 7.

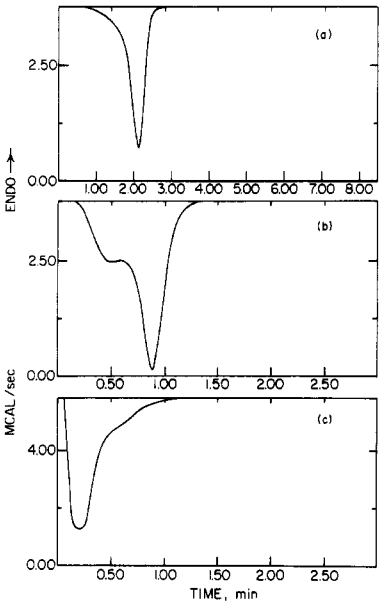

Figure 9. Isothermal crystallization experiments utilizing the exothermic method: (a) at 117 °C; (b) at 116 °C; (c) at 115 °C.

The exothermic type of isothermal crystallization experiment allows us to reduce the time scale of the crystallization studies at the expense of the detailed isotherm shape. We give examples of the isothermal exothermic results in parts a–c of Figure 9 for crystallization temperatures of 117, 116, and 115 °C, respectively. For crystallization at 117 °C, Figure 9a, only one exothermic peak is observed. On the basis of a similar study with $C_{246}H_{494}$, which was accompanied by SAXS identification,[12] this exothermic peak can be attributed to the extended crystallite form. For crystallization at 116 °C, Figure 9b, two exothermic peaks are observed. The one observed at about 0.50 min is assigned to a nonintegral, nonextended form.[12] It then develops into the extended form, which manifests itself by the major exotherm, observed at 0.89 min. The exotherm for crystallization at 115 °C, Figure 9c, indicates a major peak at 0.21 min with the beginning

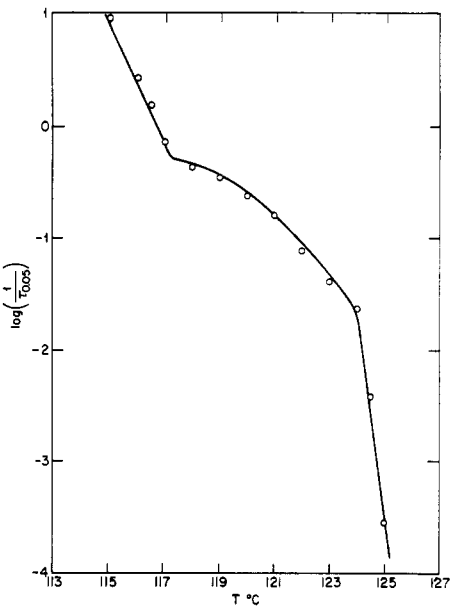

Figure 10. Crystallization rate as a function of temperature for $C_{192}H_{386}$. Plot of log $(1/\tau_{0.05})$ against temperature. $\tau_{0.05}$ is the time necessary for 5% crystallinity to develop.

of a new exotherm developing at about 0.75 min. At longer crystallization times the extended form develops completely under these conditions. These results for the rapid isothermal crystallization are comparable to those reported for $C_{246}H_{494}$ and can be interpreted in a very similar manner. Analyses of the Raman internal modes and the longitudinal acoustical modes (LAM) of $C_{192}H_{386}$ at room temperature indicate essentially complete crystallinity and the formation of extended crystallite lengths. Ungar and Keller[15] have reported a DSC cooling scan (at 40 °C/min) where a small exothermic peak at about 118 °C, attributed to the extended form, is observed followed, at slightly lower temperatures, by a large peak attributed to the formation of a nonextended form. We have performed similar rapid cooling experiments with $C_{192}H_{386}$ and have observed only the major exotherm corresponding to a nonextended form.

The crystallization rates, as evidenced by the isotherms plotted in Figure 7, display a strong negative temperature coefficient. This result is shown more strikingly in Figure 10 where both the endothermic and exothermic data are plotted. Here log $(1/\tau_{0.05})$, where $\tau_{0.05}$ is the time necessary for 5% crystallinity to develop, is plotted against the temperature. The large negative temperature coefficient, covering 5 orders of magnitude over 10 deg, is quite apparent. There appear to be three distinct regions to the plot in Figure 10. These are the low- and high-temperature regions characterized by high slopes and the intermediate region connecting these two extremes. In their study of $C_{246}H_{494}$, Ungar and Keller[15] found that in this type plot there was a maximum in the connecting region.

The strong negative temperature that is observed is very suggestive of a nucleation-controlled crystallization process. In its most general formulation, the steady-state nucleation rate N for all classes of molecular substances and nuclei types and shapes can be expressed as[43]

$$N = N_0 \exp\left(\frac{-E_0 - \Delta G^*}{RT}\right) \tag{6}$$

Here E_0 is the free energy of activation for transport across the liquid-crystal interface and ΔG^* is the free energy necessary to form a nucleus of critical size. Since ΔG^* must invariably be related to the inverse of ΔG_u, the free energy of fusion per molecule for monomeric substances,

or the corresponding free energy per repeating unit, for a chain the strong negative temperature coefficient inevitably results for nucleation in the vicinity of the melting temperature. However, despite this extremely important underlying formalism to steady-state nucleation theory, there is a fundamental difference in developing a detailed expression for low molecular weight monomeric substances as compared to chain molecules. The very important distinction that is involved depends on whether the complete molecule or only a portion thereof participates in the formation of a nucleus. This question becomes particularly important for chain molecules since in this case only a portion of the molecule participates in the nucleus.

In the classical monomeric, low molecular weight (nonchain) system the complete molecule participates in nucleus formation. In this case for a nucleus with two different surfaces, represented by interfacial free energies σ_u and σ_e, respectively, for homogeneous three-dimensional nucleation

$$\Delta G^* = \frac{8\pi\sigma_u^2\sigma_e}{\Delta G_u^2} \tag{7}$$

For a Gibbs type two-dimensional coherent nucleus

$$\Delta G^* = \frac{4\sigma_e\sigma_u}{\Delta G_u} \tag{8}$$

Other geometries and nucleation types follow a very similar pattern. It is convenient to expand ΔG_u about the actual melting point of the species, T_m, so that

$$\Delta G_u = \frac{\Delta H_u \Delta T}{T_m} \tag{9}$$

$\Delta T \equiv T_m - T$ where T is the temperature of nucleation (crystallization). Substituting eq 9 into either eq 7 or 8 allows for the evaluation of N as a function of T. The key factor here is the utilization of the melting temperature of the actual system in formulating ΔG^*.

In treating the nucleation of chain molecules, including the *n*-alkanes, cognizance must be taken of the fact that the complete molecule does not participate in the formation of the nucleus.[9] Therefore, the first step in the formation of a nucleus comprised of chain molecules involves the selection of ζ units from among the x repeating units in the chain. This selection process is a crucial step in forming the nucleus. Subsequently, additional restraints can be added to the nucleation process if deemed necessary. This problem, involving chain molecules, has been treated for both three-dimensional homogeneous nucleation and coherent two-dimensional nucleation (Gibbs type)[49,50] and can easily be extended to other types of nucleation processes. It is found that for the critical dimensions of the three-dimensional nucleus

$$\rho^{*1/2} = \frac{2\pi^{1/2}\sigma_u}{\Delta G_u - \frac{RT}{x} - \frac{RT}{(x - \zeta^* + 1)}} \tag{10}$$

$$\frac{\zeta^*}{2}\left(\Delta G_u - \frac{RT}{x} - \frac{RT}{x - \zeta^* + 1}\right) = 2\sigma_e - RT \ln\left(\frac{(x - \zeta^* + 1)}{x}\right) \tag{11}$$

$$\Delta G^* = \pi^{1/2}\zeta^*\rho^{*1/2}\sigma_u \tag{12}$$

For the two-dimensional case, the critical dimensions are

$$\rho^* = \frac{2\sigma_u}{\Delta G_u - \frac{RT}{x} - \frac{RT}{(x - \zeta^* + 1)}} \tag{13}$$

$$\zeta^* = \frac{2\sigma_e - RT \ln\left(\frac{x - \zeta^* + 1}{x}\right)}{\Delta G_u - \frac{RT}{x}} \tag{14}$$

$$\Delta G^* = \frac{2\sigma_u\left[2\sigma_e - RT \ln\left(\frac{x - \zeta^* + 1}{x}\right)\right]}{\Delta G_u - \frac{RT}{x}} = 2\sigma_u\zeta^* \tag{15}$$

Here ρ^* is the number of lateral chains involved in the nucleus, ζ^* the number of repeating units, and ΔG^* the free energy, characteristic of the critical size nucleus. Here the quantity ΔG_u is the free energy of fusion per repeating unit of the *infinite chain*. Thus

$$\Delta G_u = \frac{\Delta H_u(T_m^\circ - T)}{T_m^\circ} \tag{16}$$

where T_m° is the *equilibrium melting temperature of the infinite size chain*. The equilibrium melting temperature characteristic of the real finite chain, including the *n*-alkanes, is not directly involved in the formulation of the critical nucleus dimensions. The reason for this somewhat unusual result is that the $\zeta^*\rho^*$ units that need to be selected do not recognize the ends of the chains, except of course for the finite chain correction terms embodied in eq 10–15. Hence the usual monomeric type nucleation theory, utilizing the equilibrium melting temperatures of the species, cannot be used with chain molecules. The undercooling is not reckoned in the conventional manner since the same ΔG_u is involved for all chain lengths. This conclusion includes the *n*-alkanes since, except for the very small chain lengths, the complete molecules does not participate in the nucleation process. The error involved in adopting conventional procedures can be significant for smaller values of x but will obviously become less important at the higher molecular weights. Unfortunately, according to theory the value of ΔG^* cannot be directly applied to the analysis of experimental data without an a priori assumption of the value of σ_e. Hence, in order to analyze experimental data a selection of reasonable values must be made for this parameter.[6,9,29]

In the limit of infinite molecular weight the very interesting result is obtained in that eq 12 and 15 reduce to

$$\Delta G^* = 8\pi\sigma_u^2\sigma_e/\Delta G_u^2 \tag{17}$$

$$\Delta G^* = 4\sigma_e\sigma_u/\Delta G_u \tag{18}$$

respectively. These equations are the formulations expected from classical nucleation theory. This reduction reflects the fact that for an infinite chain there is no influence of end groups in the selection and nucleation process.

From the theory outlined, which is the basic first step in nucleating chains of finite length, we can examine the temperature coefficient data that was obtained for $C_{192}H_{386}$. We analyze the data by equating the rate constant, expressed in terms of $1/\tau_{0.05}$, to the steady-state nucleation rate. At this point we are only considering the selection contribution to the nucleation process. As has been indicated, further steps can be added to nucleus formation of deemed necessary. In this analysis we take $T_m^\circ = 145.5$ °C.[21]

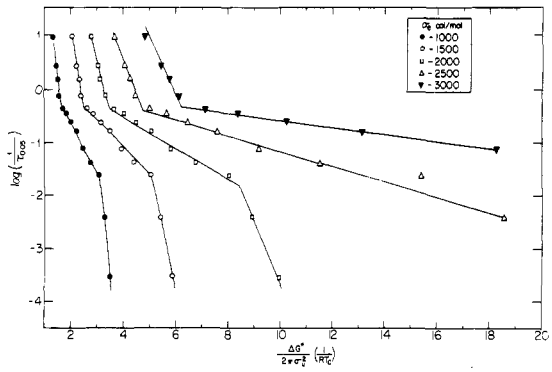

Figure 11. Treatment of crystallization kinetic data of $C_{192}H_{386}$ in terms of three-dimensional homogeneous nucleation theory.

We examine first, as an example, the case of three-dimensional homogeneous nucleation. Certain types of heterogeneous nucleation will also follow this formalism.[51] Since the appropriate values of σ_e cannot be predetermined, we need to consider a range of values for an objective analysis. The reasons for the values chosen have been discussed previously.[9] The results of treating the data according to eq 6 and 12 are plotted in Figure 11. The general characteristics of the plots depend on the value taken for σ_e. For σ_e values of 1000, 1500 and 2000 cal/mol the data are represented by three intersecting straight lines. At the temperature extremes the two straight lines are parallel to one another. For the two highest values of σ_e considered here, the experimental data are best represented by two intersecting straight lines. On the basis of the equilibrium melting temperatures of low molecular weight polyethylene fractions[6,29] and the premelting of the n-alkanes previously discussed, the lower values of σ_e would be more favored.

More detailed attention is focused on the two-dimensional coherent nucleation process. This has been the more popular type in analyzing polymer kinetics. We plot the experimental data according to eq 6 and 15 in Figure 12 for selected values of σ_e. Here the same types of results are obtained irrespective of the value chosen for σ_e. Changing the value of σ_e just shifts the data along the horizontal axis. The data plotted according to this nucleation model are very well represented by three intersecting straight lines. The straight lines representing the high- and low-temperature crystallization regions again have the same slope. The lower temperature region represents the rapid upsweep in the crystallization rate that was seen in Figure 10. Also plotted in this figure are comparable data for two low molecular weight polyethylene fractions, $M_n = 4200$ and $M_n = 5800$, that are taken from previous work.[48] We have already noted that these fractions obey Avrami type kinetics with $n = 4$, identical with the results for the n-alkane. From Figure 12 we find, depending on the value taken for σ_e, that the data points for the fractions are either identical with, or very close to, that for the n-alkane studied here. The similarities are rather striking, particularly when considering the different experimental techniques used and that two independent investigations are involved. We conclude, therefore, that there is no basic difference in the nucleation process and the overall crystallization mechanism between the two types of species. This result should in fact not be unexpected. The same number of chain units is required in the selection process for nucleus formation for either a n-alkane or a fraction of the same chain length. Put another way, in both cases the chain ends are not recognized in nucleus formation except for the correction terms. These will be similar in both cases.

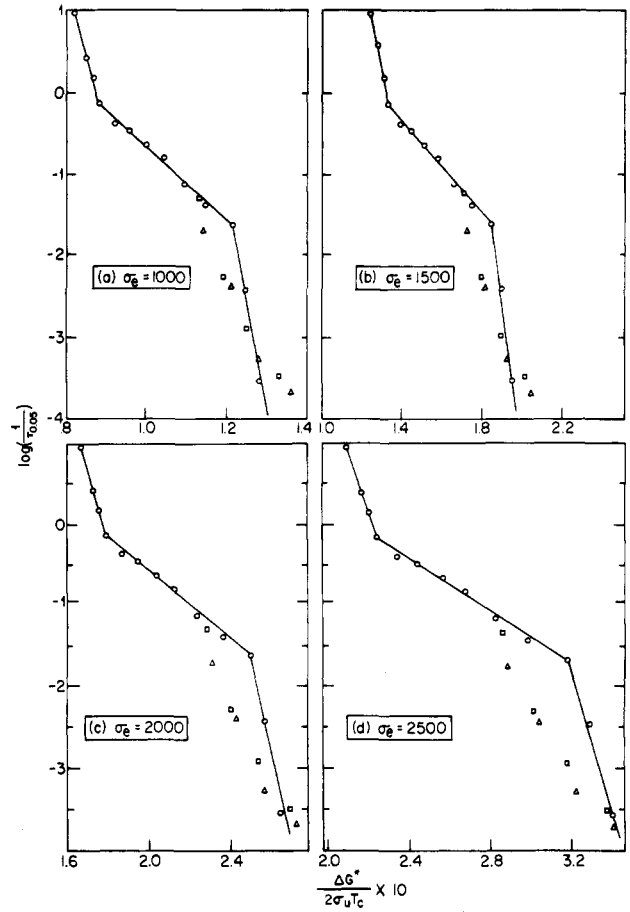

Figure 12. Treatment of crystallization kinetic data of $C_{192}H_{386}$ in terms of two-dimensional coherent nucleation theory. n-Alkane $C_{192}H_{386}$ (○). Linear polyethylene: $M = 4200$ (□); $M = 5800$ (△).

Despite the change in the nucleation pattern with temperature, which is indicated by the plots in Figure 12, extended-chain crystallites are formed in the range studied subsequent to nucleation. The observation of three intersecting straight lines is reminiscent of crystallization in regimes I–III that is observed in monomers as well as polymeric systems.[52-64] In these cases regime III, observed at low temperature, can be generalized to represent the deposition of many small nuclei and thus crystallites. In contrast at the highest temperature, regime I, the growing nucleus sweeps completely across the crystallite face before the next layer is initiated; i.e., the rate of growth from the nucleus on the surface (Gibbs type) is much faster than the nucleation rate. The temperature coefficient slope in regime III is calculated to be the same as that in regime I, which is in accord with the assignments given. In regime II additional growth steps are allowed to nucleate before the previous layer has completely covered the substrate. For coherent surface nucleation of long-chain molecules the analysis has shown that the temperature coefficient slopes are in the ratio of 0.5 between regimes II to I. The tacit assumption is made in the case of polymers that growth along the chain axis is severely retarded so that a two-dimensional growth from the nucleus takes place. Experimental results for many polymer systems, involving the measurement of either spherulitic growth or overall crystallization rates[51] appear to support the ratio of 0.5.[57-62] However, recent studies with linear polyethylene fractions encompassing a very wide molecular weight range, $M = 2 \times 10^4$–8×10^6, have shown that the slope ratios of regime II/regime I are dependent on chain length.[65] Extrapolation of the high molecular weight polymer data to $M = 2700$, corresponding to $C_{192}H_{386}$, leads to an expectation of ap-

proximately 0.3 for this ratio. We find that the corresponding ratios of slopes in Figure 12 vary from 0.23 to 0.25 depending on the value chosen for σ_e. We should also note that, in the original concept of regimes I and II developed by Hillig[52] and Calvert and Uhlman[53] for nonchainlike monomeric systems, where the growth from the nucleus along the substrate will be three-dimensional, the corresponding ratio was calculated to be 0.33. The underlying concepts of regimes I–III are thus applicable to all types of molecular species. They are not limited to long-chain molecules and *do not* require the introduction of any type of folded chain even for polymers.

With this background the possible connection between the results of Figures 11 and 12 and the classical regime concept can be examined. We have previously pointed out[9] that ζ^*, and thus ΔG^*, increases with increasing temperature so that the nucleation rate continuously decreases. Subsequent to the nucleation selection process in the *n*-alkanes, the possibility of growth along the chain axis, i.e., longitudinal or one-dimensional growth, is a key consideration. We postulate that this growth rate depends on the difference in the number of chain units between x and ζ^*. When this difference is small, growth can proceed relatively rapidly. The formation of extended-chain crystallites would thus be unimpeded. Thus, at high crystallization temmperatures we have an analogous set of conditions that stipulate the conventional regime I. Here, it is the one-dimensional longitudinal growth that is rapid relative to the nucleation process. Now as the temperature is lowered the nucleation rate increases. Concomitantly, the longitudinal growth rate will decrease since ζ^* becomes less than x. We have thus created similar conditions for conventional regime II in that multiple nucleation steps can occur prior to the completion of longitudinal growth. At still lower temperatures the very rapid nucleation rate is the major determinant of the crystallization process and leads to regime III. We thus find three regimes in the crystallization of $C_{192}H_{386}$ develop in a very natural way because of the size of the primary nucleus relative to longitudinal chain growth. This description is in accord with the temperature coefficient of the crystallization kinetics of $C_{192}H_{386}$. There is, therefore, a progression in the regime concept from a three-dimensional growth problem[52,53] to one of two-dimensional lamellar growth[54–56] and then to the current linear growth problem.

In a similar study of the crystallization kinetics of $C_{246}H_{494}$, Ungar and Keller[15] found a major difference in the temperature dependence of the crystallization rate as compared with the results for $C_{192}H_{386}$ that are reported here. Although an increase is observed in $1/\tau_{0.10}$ with the initial decrease in crystallization temperature, a maximum is observed in this function (corresponding to a minimum in the crystallization rate) followed by a rapid increase in this quantity. The crystallization kinetics of these two *n*-alkanes are thus quite different. The finite chain nucleation theory that has been described above is not adequate by itself to explain the minimum in the rate with temperature. It does, however, explain the temperature coefficient in the high-temperature region. The extremal in the crystallization rate indicates that at least two competing processes are involved in the crystallization of the higher molecular weight *n*-alkane.[66] We propose the following mechanism to explain the temperature coefficient of the crystallization kinetics of $C_{246}H_{494}$. It follows from the previous discussion of the crystallization kinetics of $C_{192}H_{386}$ and serves as a connection between the crystallization of low and high molecular weight chains.

Attention is again focused on the relationship between ζ^* and x. When ζ^* becomes very much smaller than x, longitudinal growth along the chain axis will become very slow. It is impeded by the large number of disordered, entangled chain units that must be eventually incorporated into the crystal. When this growth process becomes sufficiently slow then in order for crystallization to proceed, subsequent to primary nucleation, another growth mechanism must be involved. Under these circumstances crystallization can proceed by a lamellar growth mechanism. Since under these conditions the crystallite thickness will be much smaller than the extended-chain length, so that some type of folded-chain crystallite will result.[67] The lateral, or lamellar, growth will also be a nucleation-controlled process. The formation of a coherent Gibbs nucleus could be an example of this type. Thus in the size range where $\zeta^* \ll x$ the temperature coefficient for crystallization will be governed by a competition between longitudinal and lateral growth. The rate of nucleation for lamellar growth will continuously increase with decreasing temperature. These two types of competing crystallite growth processes will lead to an extremal in the crystallization rate consistent with nucleation control. At sufficiently low temperatures the folded-chain lamellar crystallite represents the only growth form. Being nucleation-controlled, it will rapidly increase with decreasing temperature and thus lead to the upsweep in crystallization rate with decreasing temperature. In these systems there is a long-time crystallite thickening process, which eventually leads to the extended crystallite structure.[12,14,15]

It is of interest to examine the chain length at which the proposed changes in mechanisms could take place. We consider two sets of chains: one of low molecular weight, $x \leq 100$, and the other of high molecular weight, $x \geq 500$. In the former case ζ^* will always be comparable to x at all crystallization temperatures, for reasonable values of σ_e, and extended-chain crystallites will be formed.[9] On the other hand, in the high molecular weight region ζ^* will always be very much less than x, and a folded-chain lamellar crystallite results for the reasons previously discussed. These changes in crystallization mechanisms can be expected to occur in the regions approximated by x = 200–300.[9] We have already noted that $C_{192}H_{386}$ only forms extended crystallites in the range of crystallization temperatures studied. Thus the primary type nucleation theory is followed quite well. On the other hand, while the higher homologue $C_{246}H_{494}$ follows this type of nucleation process at high crystallization temperatures the onset of a folded-chain type crystallite at lower temperatures involves an additional type of nucleation. The concepts that have been outlined above, which admittedly have many qualitative features, serve as a connection between the crystallization of low molecular weight chains and high moleceular weight polymers. In long chains only a folded type lamellar structure is found because of the very retarded crystallite thickening rate.[68,69]

Summary

In studying the major aspects of the crystallization behavior of the high molecular weight *n*-alkane $C_{192}H_{386}$, several fundamental features concerned with both the fusion and crystallization process have emerged. Although at room temperature complete crystallinity, consistent with the formation of molecular crystals, is observed, premelting is found at elevated temperatures prior to complete melting. This conclusion is shown to be consistent with the Flory–Vrij[23] analysis and other data on the *n*-alkanes existing in the literature. A reexamination of the melting temperature–chain length relation of the *n*-alkanes, to take

into account the possibilities of premelting, is indicated.

Studies of the crystallization kinetics from the pure melt reveal that a classical crystallization process is taking place where the Avrami type analysis is followed. The temperature coefficient of the crystallization indicates that it is nucleation-controlled and follows the theory developed for chains of finite molecular weight. Literature data for a higher molecular weight homologue yields a more complex temperature coefficient, which can be accounted for by competing crystallization processes. The connection between the crystallization of low and high molecular weight chains becomes clear from these results and analyses.

Acknowledgment. Support of this work at Florida State University by the National Science Foundation Polymers Program Grant DMR 86-13007 is gratefully acknowledged. We also thank A. Reichert and F. P. Gramlich for their skillful preparation of the compound studied.

Registry No. $C_{192}H_{386}$, 96123-38-5.

References and Notes

(1) Paynter, D. I.; Simmonds, D. J.; Whiting, M. C. *J. Chem. Soc., Chem. Commun.* **1982**, 1165.
(2) Bidd, I.; Whiting, M. C. *J. Chem. Soc., Chem. Commun.* **1985**, 542.
(3) Lee, K. S.; Wegner, G. *Macromol. Chem., Rapid Commun.* **1985**, *6*, 203.
(4) Kloos, F.; Go, S.; Mandelkern, L. *J. Polym. Sci.* **1974**, *12*, 1145.
(5) Leung, W. M.; Manley, R. St. J.; Panaras, A. R. *Macromolecules* **1985**, *18*, 760.
(6) Stack, G. M.; Mandelkern, L.; Voigt-Martin, I. G. *Macromolecules* **1984**, *17*, 321.
(7) Kloos, F.; Go, S.; Mandelkern, L., unpublished results.
(8) Prasad, A.; Mandelkern, L. *Macromolecules* **1989**, *22*, 914.
(9) Stack, G. M.; Mandelkern, L. *Macromolecules* **1988**, *21*, 510.
(10) Ungar, G.; Stejny, J.; Keller, A.; Bidd, I.; Whiting, M. C. *Science (Washington, D.C.)* **1985**, *229*, 386.
(11) Hoffman, J. D. *Polym. Commun.* **1986**, *27*, 39.
(12) Ungar, G.; Keller, A. *Polymer* **1986**, *27*, 1835.
(13) Ungar, G.; Keller, A. *Polym. Commun.* **1987**, *28*, 232.
(14) Organ, S. J.; Keller, A. *J. Polym. Sci., Polym. Phys. Ed.* **1987**, *25*, 2409.
(15) Ungar, G.; Keller, A. *Polymer* **1987**, *28*, 1899.
(16) Lee, K. S. Thesis, Freiburg, FRG, 1984.
(17) Lee, K. S.; Wegner, G.; Hsu, S. C. *Polymer* **1987**, *28*, 889.
(18) Strobl, G. R.; Hagedorn, W. *J. Polym. Sci., Polym. Phys. Ed.* **1978**, *16*, 1181.
(19) Glotin, M.; Mandelkern, L. *Colloid Polym. Sci.* **1982**, *260*, 182.
(20) Mandelkern, L.; Peacock, A. J. *Polym. Bull.* **1986**, *16*, 529.
(21) Mandelkern, L.; Peacock, A. J., to be submitted for publication.
(22) Mandelkern, L.; Stack, G. M. *Macromolecules* **1984**, *17*, 871.
(23) Flory, P. J.; Vrij, A. *J. Am. Chem. Soc.* **1963**, *85*, 3548.
(24) Mandelkern, L. Crystallization and Melting of Polymers. In *Comprehensive Polymer Science, Polymer Properties*; Booth, C., Price, C., Eds.; Pergamon: New York, 1989; Vol. 2.
(25) Möller, M.; Cantow, H. J.; Drotloff, H.; Emeis, D.; Lee, K. S.; Wegner, G. *Makromol. Chem.* **1986**, *187*, 1237.
(26) Hay, J. N. *J. Polym. Sci., Part B* **1970**, *8*, 395.
(27) Takimizawa, K.; Ogawa, Y.; Oyama, T. *Polym. J.* **1982**, *14*, 441.
(28) Sullivan, P. K.; Weeks, J. J. *J. Res. Natl. Bur. Stand.* **1970**, *74A*, 203.
(29) Mandelkern, L.; Prasad, A.; Stack, G. M., to be submitted for publication.
(30) Ubbelohde, A. R. *The Molten State of Matter*; John Wiley: New York, 1978; p 321 ff.
(31) Heitz, W.; Wirth, Th.; Peters, R.; Strobl, G.; Fischer, G. W. *Makromol. Chem.* **1972**, *162*, 63.
(32) Strobl, G. R. *J. Polym. Sci., Polym. Symp.* **1977**, *59C*, 121.
(33) Broadhurst, M. G. *J. Res. Natl. Bur. Stand.* **1962**, *66A*, 241.
(34) Quinn, F. A., Jr.; Mandelkern, L. *J. Am. Chem. Soc.* **1958**, *80*, 3178.
(35) Mandelkern, L.; Stack, G. M.; Mathieu, P. J. *Anal. Calorim.* **1984**, *5*, 223.
(36) Alamo, R.; Mandelkern, L. *J. Polym. Sci., Polym. Phys. Ed.* **1986**, *24*, 2087.
(37) Mandelkern, L. *Crystallization of Polymers*; McGraw-Hill: New York, 1964; p 321 ff.
(38) Hoffman, J. D.; Weeks, J. J. *J. Res. Natl. Bur. Stand.* **1962**, *66A*, 13.
(39) Flory, P. J. *J. Chem. Phys.* **1949**, *17*, 223.
(40) Obviously longer time scales at higher temperatures could be studied, which would, however, involve an inordinate investment of time.
(41) Here we have taken the theoretical value of 940 cal/mol for complete transformation to molecular crystals. The results and conclusions are not essentially changed if we use the highest value observed here for ΔH_u.
(42) Avrami, M. *J. Chem. Phys.* **1939**, *7*, 1103; *Ibid.* **1940**, *8*, 212; *Ibid.* **1941**, *9*, 177.
(43) Reference 29, p 215 ff.
(44) Mandelkern, L.; Quinn, F. A., Jr.; Flory, P. J. *J. Appl. Phys.* **1954**, *25*, 830.
(45) Ergoz, E.; Fatou, J. G.; Mandelkern, L. *Macromolecules* **1972**, *5*, 147.
(46) Von Göler, F.; Sachs, G. *Z. Phys.* **1932**, *77*, 281.
(47) For long-chain molecules it is often convenient to consider the crystallization on a normalized basis to allow for the restricted level of crystallinity that can be eventually attained.
(48) Ergoz, E. Ph.D. Dissertation, Florida State University, 1970.
(49) Fatou, J. G.; Howard, C.; Mandelkern, L. *J. Phys. Chem.* **1964**, *68*, 3386.
(50) Mandelkern, L.; Fatou, J. G.; Howard, G. *J. Phys. Chem.* **1965**, *69*, 956.
(51) Devoy, C.; Mandelkern, L. *J. Chem. Phys.* **1970**, *52*, 3827.
(52) Hillig, W. G. *Acta Metall.* **1966**, *14*, 1868.
(53) Calvert, P. D.; Uhlman, D. R. *J. Appl. Phys.* **1972**, *43*, 1944.
(54) Sanchez, I. C.; DiMarzio, E. A. *Macromolecules* **1971**, *4*, 677.
(55) Sanchez, I. C.; DiMarzio, E. A. *J. Res. Natl. Bur. Stand.* **1972**, *76A*, 213.
(56) Lauritzen, J. I., Jr. *J. Appl. Phys.* **1973**, *44*, 4353.
(57) Maxfield, J.; Mandelkern, L. *Macroomolecules* **1977**, *10*, 1141.
(58) Hoffman, J. D.; Frolen, L. J.; Ross, G. S.; Lauritzen, J. I., Jr. *J. Res. Natl. Bur. Stand.* **1975**, *79A*, 671.
(59) Alamo, R.; Fatou, J. G.; Guzman, J. *Polymer* **1982**, *23*, 379.
(60) Allen, R. C.; Mandelkern, L. *Polym. Bull.* **1987**, *17*, 473.
(61) Monasse, B.; Haudin, J. M. *Colloid Polym. Sci.* **1985**, *263*, 822.
(62) Phillips, P. J.; Vatansever, N. *Macromolecules* **1987**, *20*, 2138.
(63) Hoffman, J. D. *Polymer* **1985**, *26*, 803.
(64) Frank, F. C. *J. Cryst. Growth* **1974**, *22*, 233.
(65) Fatou, J. G.; Marco, C.; Mandelkern, L., submitted for publication.
(66) Maximum in crystallization rates quite often observed in polymers can be attributed in a straightforward manner to a competition between the transport term as the glass temperature is approached and the nucleation rate. This explanation is obviously not appropriate in the present case.
(67) We use the expression "folded-chain crystallites" to convey the idea that the crystallite thickness is not comparable to the extended-chain length. In this sense the word folded is used properly. There is no implication here as to the nature of the interfacial structure of the basal plane and the details of the folding. It must not be assumed that the nucleation involves regularly folded chains.
(68) Stack, G. M.; Mandelkern, L.; Voigt-Martin, I. G. *Polym. Bull.* **1982**, *8*, 421.
(69) Stack, G. M. Ph.D. Dissertation, Florida State University, 1987.